# Geometric Vacuum Selection from Constrained Spacetime Foliations

Michael Spina

`michael.spina@mail.com`

February 21, 2026

## Abstract

We investigate a scalar-field framework for vacuum structure in General Relativity, in which the foliation defined by the gradient of a time-ordering field $\Theta$ is subject to a non-local geometric constraint. The level sets $\Theta = \text{const}$ define spacelike hypersurfaces interpreted as physical "present" leaves. The constraint fixes the asymptotic normalized average of the squared extrinsic curvature in the infrared limit to a constant scale $K_0^2$, enforced by a leafwise-constant Lagrange multiplier $\lambda(\Theta)$.

We show that this non-local condition acts as a vacuum-selection principle: in the infrared limit it generically excludes the static Minkowski vacuum, compelling the ground state to be spontaneously curved. De Sitter spacetime emerges as a consistent asymptotic vacuum solution, with its expansion rate fixed by the geometric selection rule $H^2 = K_0^2/3$.

We further demonstrate that the infrared dominance of the constraint ensures compatibility with local gravitational physics. Standard Schwarzschild and post-Newtonian limits are recovered for local sources, as the constraint does not introduce unsuppressed local modifications of the gravitational dynamics.

These results suggest that the observed late-time cosmic acceleration may reflect a global geometric property of the spacetime foliation—a resistance to staticity—rather than the presence of an additional dynamical dark energy degree of freedom. A supplementary minisuperspace check including barotropic matter shows that, under a hard implementation of the leafwise constraint, the selected homogeneous branch remains de Sitter ($H^2 = K_0^2/3$) while matter sources the leafwise multiplier $\lambda(\Theta)$ rather than an evolving $H(t)$. This reinforces the need for a finite-domain/causal prescription to obtain a realistic radiation/matter history.

**Conventions**

We work in natural units $c = \hbar = 1$ adopting metric signature $(+, -, -, -)$. Our curvature conventions follow

$$R^{\rho}{}_{\sigma\mu\nu} = \partial_{\mu}\Gamma^{\rho}_{\nu\sigma} - \partial_{\nu}\Gamma^{\rho}_{\mu\sigma} + \Gamma^{\rho}_{\mu\lambda}\Gamma^{\lambda}_{\nu\sigma} - \Gamma^{\rho}_{\nu\lambda}\Gamma^{\lambda}_{\mu\sigma}, \qquad R_{\mu\nu} = R^{\rho}{}_{\mu\rho\nu}. \quad (1)$$

For the nonlocal functional we set the smoothing/window parameter to its default value $W = 1$ throughout (no variation with respect to $W$ is performed).

# 1 Motivation and scope

General Relativity provides an accurate local description of gravitational phenomena, yet it leaves the global structure of time and the selection of the vacuum largely unconstrained. In particular, both Minkowski and de Sitter spacetimes are admissible vacuum solutions, despite their radically different global properties. The observed accelerated expansion is therefore introduced phenomenologically through a cosmological constant, rather than emerging from a geometric principle.

In this work we explore a minimal geometric extension of General Relativity based on a scalar field $\Theta$ whose timelike gradient defines a preferred foliation of spacetime. Preferred-foliation frameworks closely related in spirit include Einstein–Æther and khronometric theories, where a timelike vector (or scalar-defined) structure selects a preferred slicing while remaining compatible with standard local tests in appropriate limits [1, 2, 3, 4]. The level sets $\Theta = \text{const}$ are interpreted as physical "present" hypersurfaces, providing a global time-ordering structure without affecting local causal relations or observer-dependent simultaneity.

The central ingredient is a non-local geometric constraint acting on the foliation itself: the normalized average of the squared extrinsic curvature $K^2$ over a causally defined domain on each hypersurface is fixed to a constant value. This leafwise constraint selects the global vacuum geometry without introducing unsuppressed local modifications of the gravitational dynamics.

We show that asymptotically flat Minkowski spacetime is not generically selected as an infrared vacuum, while de Sitter spacetime is admitted as a consistent asymptotic solution, with its expansion rate fixed by the constraint. Local Schwarzschild and post-Newtonian physics are recovered, as the constraint is dominated by infrared scales.

The purpose of this work is not to present a complete modified-gravity theory valid at all scales, nor a full cosmological model including perturbations and matter evolution. Rather, the framework is intended as a proof-of-principle demonstrating how a non-local, foliation-based geometric constraint can act as an infrared vacuum-selection mechanism within General Relativity.

While the present manuscript focuses on the strict infrared vacuum-selection mechanism and its consistency with local GR limits, we also provide a dedicated supplementary pipeline (`Perturbative_Spectrum_Study`, scripts 00–15) that derives the quadratic kernel around isotropic backgrounds and evaluates ghost/gradient stability conditions in the tensor, vector and scalar (mixing) sectors, including the infrared suppression expected from the normalized-channel structure. A full BRST/Faddeev–Popov proof of gauge-independence of physical residues, a fundamental UV cutoff/UV completion, and a complete cosmological-perturbation phenomenology remain outside the scope of this work.

**Additional supplementary minisuperspace pipeline (barotropic matter).** We additionally provide a dedicated supplementary minisuperspace pipeline (`Paper/Barotropic_Cosmology_Study`) analyzing FRW cosmology with barotropic matter. It verifies that on the hard-constrained homogeneous branch (by "hard implementation" we mean a uniform enforcement of the infrared leafwise condition $Q(\theta) = K_0^2$ across all leaves in the homogeneous reduction, rather than a finite-domain/causal prescription) the constraint fixes $H^2 = K_0^2/3$ while the matter sector is absorbed into a time-dependent leafwise multiplier $\lambda(\Theta)$, thereby motivating the finite-domain/causal formulation required for a realistic radiation/matter era.

## 2  Geometric setup

We consider a four-dimensional spacetime $(\mathcal{M}, g_{\mu\nu})$ endowed with a scalar field $\Theta$. When the gradient $\nabla_\mu \Theta$ is timelike, the level sets $\Theta = \mathrm{const}$ define a foliation of spacetime by spacelike hypersurfaces $\Sigma_\Theta$. Scalar fields used to define preferred time functions and associated foliations in GR have been considered in earlier contexts; see e.g. [5]. Throughout this work, we restrict attention to configurations satisfying this condition.

The scalar invariant

$$X \equiv g^{\mu\nu} \partial_\mu \Theta \, \partial_\nu \Theta \tag{2}$$

is assumed to be positive, ensuring that $\nabla_\mu \Theta$ is timelike. We then define the unit normal vector field to the foliation as

$$u_\mu \equiv \frac{\partial_\mu \Theta}{\sqrt{X}} \, . \tag{3}$$

The induced metric on each hypersurface $\Sigma_\Theta$ is given by

$$h_{\mu\nu} \equiv g_{\mu\nu} - u_\mu u_\nu, \tag{4}$$

which projects tensors onto directions tangent to the foliation. We denote by $\gamma_{ij}$ the (positive-definite) induced three-metric on each leaf $\Sigma_\Theta$. Its determinant is $\gamma \equiv \det(\gamma_{ij})$, and the intrinsic volume element is $\sqrt{\gamma} \, d^3x$. The

extrinsic curvature of the hypersurfaces is defined in the standard way as

$$K_{\mu\nu} \equiv h^{\alpha}{}_{\mu} h^{\beta}{}_{\nu} \nabla_{\alpha} u_{\beta}. \tag{5}$$

A key scalar quantity in what follows is the squared extrinsic curvature,

$$K^2 \equiv K_{\mu\nu} K^{\mu\nu}, \tag{6}$$

which measures the curvature of the $\Theta = \text{const}$ hypersurfaces within spacetime. Together with the Ricci scalar $R$ of the spacetime metric, these invariants will enter the action and the geometric constraint introduced in later sections.

# 3 Spherically symmetric sector

In order to analyze the geometric properties of the $\Theta$-foliation and to construct explicit examples, we consider a static, spherically symmetric spacetime. The metric is written in the form

$$ds^2 = A(r) \, dt^2 - B(r) \, dr^2 - r^2 \left( d\vartheta^2 + \sin^2 \vartheta \, d\varphi^2 \right), \tag{7}$$

where $A(r)$ and $B(r)$ are positive functions of the radial coordinate.

For the scalar field we adopt the ansatz

$$\Theta(t, r) = t + \psi(r), \tag{8}$$

which preserves spherical symmetry while allowing for nontrivial foliations tilted with respect to the static time coordinate. This form captures the most general $\Theta$ compatible with the symmetries of the metric.

## 3.1 Kinematic invariant

For the above ansatz, the kinetic scalar $X$ takes the form

$$X = \frac{1}{A(r)} - \frac{\psi'(r)^2}{B(r)}. \tag{9}$$

The requirement that the foliation be spacelike implies $X > 0$, which constrains the admissible profiles $\psi(r)$.

## 3.2 Curvature invariants

The Ricci scalar associated with the metric is given by

$$R = R[A(r), B(r)], \tag{10}$$

where the explicit expression, though lengthy, depends only on the radial functions and their derivatives.

The squared extrinsic curvature of the $\Theta = \text{const}$ hypersurfaces can be written as

$$K^2 = K_{\mu\nu}K^{\mu\nu} = K^2\big(A(r), B(r), \psi(r), \psi'(r), \psi''(r)\big). \qquad (11)$$

The explicit form is algebraically involved and will not be reproduced in full here. What is important for our purposes is its dependence on the radial coordinate through the functions $A(r)$, $B(r)$ and the foliation profile $\psi(r)$.

These local expressions will enter the construction of the action and the leafwise geometric constraint discussed in the following sections.

## 4 Constrained action

### 4.1 Local gravitational dynamics

We start from a local action consisting of the Einstein–Hilbert term and a minimal kinetic term for the scalar field $\Theta$,

$$S_{\text{loc}} = \int d^4x \sqrt{-g} \left[ \frac{1}{2\kappa}(R - 2\Lambda) - \frac{\alpha}{2} X \right], \qquad (12)$$

where $\kappa = 8\pi G$, $\Lambda$ is a cosmological constant and $X = g^{\mu\nu}\partial_\mu\Theta\,\partial_\nu\Theta$. We take the scalar field $\Theta$ to have dimensions of length (time in units $c = 1$), so that $\partial_\mu\Theta$ is dimensionless and the kinetic scalar $X$ is dimensionless. Accordingly, the coupling constant $\alpha$ has dimensions $[L^{-4}]$. Although the local action includes a standard kinetic term for the scalar field $\Theta$, this term is not introduced to model an additional physical scalar degree of freedom. Rather, $\Theta$ plays the role of a geometric time-ordering field whose gradient defines the spacetime foliation on which the non-local constraint acts. The kinetic term should therefore be understood as a regulator enforcing the timelike character of $\nabla_\mu\Theta$ and the regularity of the foliation. In the infrared regime of interest, the dynamics of $\Theta$ is dominated by the leafwise constraint, and the theory approaches a non-propagating, cuscuton-like limit. A detailed analysis of the scalar mode content is left for future investigation. This local action is fully diffeomorphism invariant and does not introduce any preferred frame by itself.

**On the bare cosmological constant.** We keep $\Lambda$ explicit for generality. In the vacuum-selection discussion below we set the bare value to $\Lambda = 0$, so that the de Sitter curvature scale arises from the leafwise constraint as a selection rule rather than being put in by hand.

### 4.2 Leafwise geometric constraint

The defining ingredient of the theory is a non-local geometric constraint acting on the foliation defined by $\Theta$. For each hypersurface $\Sigma_\Theta$ we consider

a causally defined domain $D_\Theta \subset \Sigma_\Theta$, determined by the spacetime geometry and the foliation itself.

Throughout this work, the causal domain $D_\Theta$ is defined as the maximal causally accessible region of the hypersurface $\Sigma_\Theta$, i.e. the largest connected subset of $\Sigma_\Theta$ whose points are mutually related by causal curves in the ambient spacetime geometry. This definition is intrinsic to the foliation and does not depend on the choice of any fiducial observer. In asymptotically flat spacetimes, $D_\Theta$ extends to spatial infinity, while in spacetimes with a cosmological horizon the causal domain is bounded by the horizon scale, providing a finite and geometrically natural infrared cutoff.

On each leaf we define the functionals

$$I_0[\Theta] \equiv \int_{D_\Theta} W \sqrt{\gamma}\, d^3x, \qquad I_1[\Theta] \equiv \int_{D_\Theta} W\, K^2 \sqrt{\gamma}\, d^3x, \qquad (13)$$

where $\gamma$ is the determinant of the induced three-metric $\gamma_{ij}$ on $\Sigma_\Theta$, and $W \geq 0$ is an optional smoothing/window weight (set to $W = 1$ in this work). Then

$$\langle K^2 \rangle_{D_\Theta} \equiv \frac{I_1[\Theta]}{I_0[\Theta]}. \qquad (14)$$

The geometric constraint is imposed by requiring

$$\lim_{R \to \infty} \frac{\int_{D_\Theta(R)} K^2 \sqrt{\gamma}\, d^3x}{\int_{D_\Theta(R)} \sqrt{\gamma}\, d^3x} = K_0^2, \qquad (15)$$

where $K_0$ is a fixed parameter setting the curvature scale of the foliation. Here, $D_\Theta(R)$ denotes a family of nested subdomains monotonically exhausting $D_\Theta$ as $R \to \infty$. In spacetimes where $D_\Theta$ is itself bounded (e.g. by a cosmological horizon), the limit is saturated at finite $R$ and the constraint is automatically well-defined without external regulators. Conceptually, the use of global (or nonlocal) constraints to control vacuum properties has precedents in unimodular formulations and vacuum-energy sequestering mechanisms[1]. The present constraint, however, acts on a foliation-dependent extrinsic-curvature functional rather than on the metric determinant or on matter-sector vacuum contributions.

## 4.3 Full action

The constraint is enforced through a leafwise-constant Lagrange multiplier $\lambda(\Theta)$ that depends only on the value of the scalar field and is therefore constant on each hypersurface $\Sigma_\Theta$. The full action reads

$$S = S_{\text{loc}} + \int d\Theta\, \lambda(\Theta) \left[ I_1[\Theta] - K_0^2 I_0[\Theta] \right]. \qquad (16)$$

---

[1]...

With $[\Theta] = L$, the leafwise Lagrange multiplier $\lambda(\Theta)$ has dimensions $[L^{-2}]$, ensuring that the non-local contribution to the action is dimensionless. Because $\lambda$ is not a local field but a function of $\Theta$ only, the constraint does not generate a pointwise equation $K^2(x) = K_0^2$. Instead, it acts globally on the geometry of each leaf, selecting admissible foliations without introducing unsuppressed local modifications of the gravitational dynamics. Boundary terms required for a well-defined variational principle can be made explicit by representing the causal domain through an indicator function and performing a covariant shape variation; the full covariant treatment is given in Appendix A. A complete bulk+boundary derivation of the non-local Euler–Lagrange structure is provided in the supplementary `Variational_Derivation` pipeline (scripts 00–25), together with symbolic and independent numerical checks.

## 4.4 Variational structure and infrared dominance

A complete derivation of the Euler–Lagrange structure associated with the non-local term in (16) is now available in the supplementary `Variational_Derivation` pipeline (scripts 00–25) and is summarized in covariant form in Appendix A, including explicit bulk/boundary splitting and independent numerical cross-checks. Here we summarize the structural features needed in the main text.

Define the leafwise functionals

$$I_0[\Theta] \equiv \int_{D_\Theta} W \sqrt{\gamma}\, d^3x, \qquad I_1[\Theta] \equiv \int_{D_\Theta} W K^2 \sqrt{\gamma}\, d^3x,$$
$$Q[\Theta] \equiv \frac{I_1[\Theta]}{I_0[\Theta]} = \langle K^2 \rangle_{D_\Theta}. \tag{17}$$

For an arbitrary first-order variation one has the exact ratio identity

$$\delta Q = \frac{I_0\, \delta I_1 - I_1\, \delta I_0}{I_0^2}. \tag{18}$$

This formula underlies both the constraint channel and the metric/scalar Euler–Lagrange channels and is repeatedly used in the supplementary derivation.

Crucially, when the domain $D_\Theta$ is treated as a *geometrically defined* region, its variation contributes alongside the usual bulk variations. Writing schematically

$$\delta I_a = \delta I_a^{\text{bulk}} + \delta I_a^{\partial D} \qquad (a = 0, 1), \tag{19}$$

the induced boundary piece in the normalized channel is

$$\delta Q\big|_{\partial D} = \frac{b_1\, I_0 - b_0\, I_1}{I_0^2}, \tag{20}$$

where $b_0, b_1$ are the domain-shape ("injection") densities associated with $I_0$ and $I_1$ on $\partial D_\Theta$. In the covariant formulation (supplementary scripts 23–25), this term arises from a shape derivative $\delta \chi_\Theta \sim \rho \, \delta(\partial D_\Theta)$ of the causal-domain indicator $\chi_\Theta$, i.e. it is not added by hand.

Equation (18) immediately implies infrared dominance in the normalized channel: for extensive variations $\delta I_a = \mathcal{O}(I_0)$ one has

$$\delta Q = \mathcal{O}\left(\frac{1}{I_0}\right), \tag{21}$$

so the induced corrections to the local field equations are suppressed by inverse powers of the leafwise volume. In asymptotically flat configurations $I_0 \sim L^3$ for a domain of linear size $L$, and the non-local corrections vanish locally as $L \to \infty$. In spacetimes with a cosmological horizon, $D_\Theta$ saturates at finite size, so the same mechanism naturally selects an infrared vacuum geometry while leaving local Schwarzschild/post-Newtonian physics unsuppressed at leading order.

## 5 Sanity checks and local GR recovery

### 5.1 Schwarzschild test

As a first consistency check, we evaluate the curvature invariants for the Schwarzschild solution,

$$A(r) = 1 - \frac{2M}{r}, \qquad B(r) = \left(1 - \frac{2M}{r}\right)^{-1}. \tag{22}$$

The Ricci scalar vanishes identically,

$$R\big|_{\text{Schw}} = 0, \tag{23}$$

as expected for a vacuum solution of General Relativity. Crucially, the existence of this solution is not obstructed by the leafwise constraint. Since the geometric condition (15) is defined as an asymptotic limit $R \to \infty$, the contributions from local matter distributions or compact objects like black holes are suppressed by the infinite volume of the integration domain. Consequently, the theory does not introduce unsuppressed local modifications of the gravitational dynamics. The recovery of standard weak-field and post-Newtonian behavior in the presence of preferred-structure fields follows from this infrared dominance, analogous to established results in Einstein–Æther theory; see e.g. [2] for explicit equivalence proofs

## 5.2 Static foliation limit

When the foliation coincides with constant-$t$ hypersurfaces ($\psi = $ const), the scalar invariants reduce to

$$X\big|_{\psi'=0} = \frac{1}{A(r)}, \tag{24}$$

$$K^2\big|_{\psi'=0} = 0. \tag{25}$$

In this static limit, the extrinsic curvature of the $\Theta$-hypersurfaces vanishes identically. However, compatibility with General Relativity holds more generally. For generic asymptotically flat foliations where $K^2$ may be non-vanishing near the source, the contribution to the global average scales as the ratio of a finite strong-field volume to the infinite integration volume. In the limit $R \to \infty$, local sources effectively represent measure-zero corrections to the vacuum selection rule. This confirms that the global constraint acts purely as an infrared boundary condition, leaving local astrophysical tests of gravity unaffected. The static identities above are also certified in the Lean artifact by the static-limit lemmas in `StaticSanityCheck/StaticLimit.lean`.

# 6 Vacuum selection from the leafwise constraint

## 6.1 Minkowski spacetime

We now evaluate the leafwise geometric functional for Minkowski spacetime, written in static spherical coordinates,

$$A(r) = 1, \qquad B(r) = 1. \tag{26}$$

For foliations of the form $\Theta = t + \psi(r)$ the kinetic invariant becomes

$$X = 1 - \psi'(r)^2, \tag{27}$$

so that the timelike condition requires $|\psi'(r)| < 1$.

For a linear tilt $\psi(r) = vr$, one finds

$$K^2(r) = \frac{2v^2}{r^2(1 - v^2)}, \tag{28}$$

which is strictly positive but decays as $r^{-2}$ at large radius.
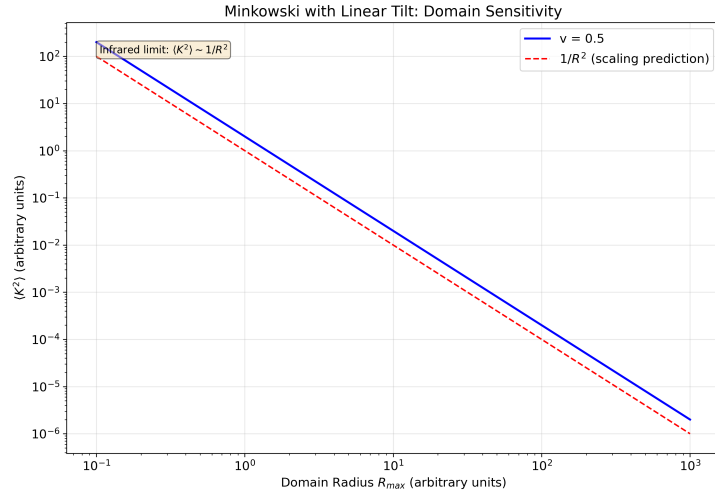
## 6.2 Infrared behaviour of the leafwise average

The leafwise constraint does not involve the pointwise value of $K^2(r)$, but its normalized average over a causally defined domain $D_\Theta$,

$$\langle K^2 \rangle_{D_\Theta} = \frac{\int_{D_\Theta} W \, K^2 \sqrt{\gamma} \, d^3x}{\int_{D_\Theta} W \sqrt{\gamma} \, d^3x}. \tag{29}$$

In Minkowski spacetime, the induced volume element grows as $\sqrt{\gamma} \sim r^2$, while $K^2 \sim r^{-2}$. As a consequence, the numerator scales linearly with the infrared cutoff, whereas the denominator grows cubically. In the infrared limit one therefore finds
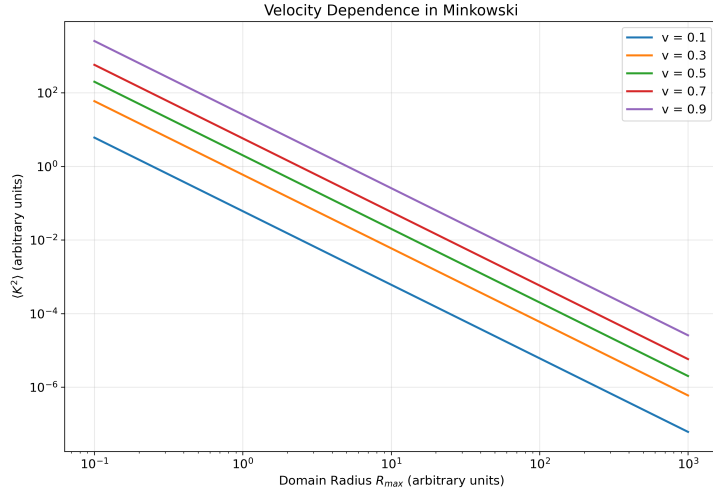
$$\langle K^2 \rangle_{D_\Theta} \xrightarrow{\text{IR}} 0. \tag{30}$$

In Lean, this infrared statement is certified by the Minkowski IR-limit theorem in `StaticSanityCheck/MinkowskiLinearTilt.lean`.
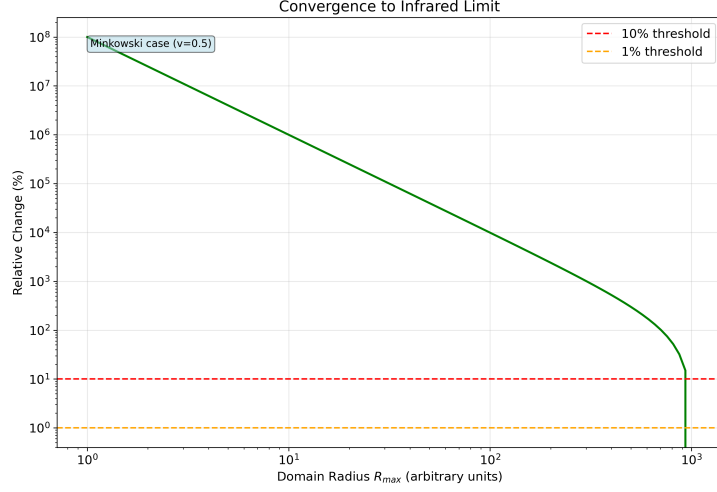


**Figure 1:** Infrared behaviour of the leafwise average $\langle K^2 \rangle$ in Minkowski spacetime with linear tilt. The numerical scaling confirms $\langle K^2 \rangle \propto R_{\max}^{-2}$, implying a vanishing average extrinsic-curvature invariant in the infrared limit $R_{\max} \to \infty$.

This result holds independently of the tilt parameter $v$ and reflects a purely geometric scaling property of asymptotically flat spacetime.

**Figure 2:** Dependence of $\langle K^2 \rangle$ on the foliation tilt parameter $v$ in Minkowski spacetime (evaluated at finite infrared cutoffs). While the overall amplitude depends on $v$, the infrared decay with increasing $R_{\max}$ and the limit $\langle K^2 \rangle \to 0$ are universal, supporting the generic exclusion of Minkowski as an infrared vacuum for $K_0^2 > 0$.

This infrared scaling mechanism is qualitatively reminiscent of other approaches where large-scale (IR) effects can drive late-time acceleration without introducing a new local dark-energy field, albeit implemented here as a geometric selection rule rather than as a dynamical nonlocal modification of the field equations [6]. Therefore, for generic asymptotically flat foliations whose extrinsic curvature decays at large radius, Minkowski spacetime cannot satisfy the leafwise constraint $\langle K^2 \rangle_{D_\Theta} = K_0^2$ for any $K_0^2 > 0$. This result follows from the infrared scaling of the normalized average and is independent of the specific tilt parameters of the foliation. While special constant-mean-curvature or hyperboloidal slicings of flat spacetime may evade this argument by enforcing a non-vanishing extrinsic curvature through global boundary conditions, such configurations require fine-tuned foliation choices and do not arise generically from the infrared-dominated causal domains considered here. In this sense, Minkowski spacetime is not selected as a natural infrared vacuum by the leafwise geometric constraint.

11

**Figure 3:** Convergence of the Minkowski leafwise average $\langle K^2 \rangle (R_{\max})$ toward its infrared limit (example shown for $v = 0.5$). The plot illustrates that a genuinely infrared domain is required for robust convergence, motivating the interpretation of the constraint as an infrared boundary condition defined by horizon-scale causal domains.

## 6.3 de Sitter spacetime

We next consider de Sitter spacetime in the static patch,

$$A(r) = 1 - H^2 r^2, \qquad B(r) = \left(1 - H^2 r^2\right)^{-1}. \tag{31}$$

For the Painlevé–Gullstrand slicing,

$$\psi'(r) = \frac{Hr}{1 - H^2 r^2}, \tag{32}$$

the kinetic invariant satisfies $X = 1$, and the squared extrinsic curvature of the $\Theta$-hypersurfaces is constant,
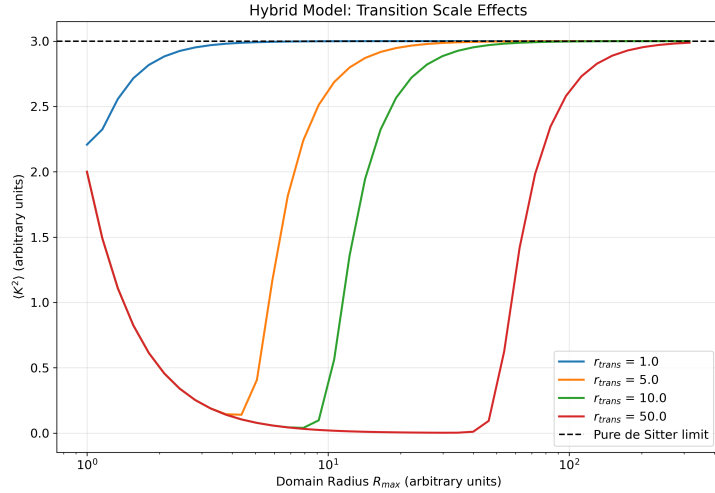
$$K^2 = 3H^2. \tag{33}$$

Since $K^2$ is constant on the entire causal domain of the static patch, its normalized leafwise average coincides with the local value,

$$\langle K^2 \rangle_{D_\Theta} = 3H^2. \tag{34}$$

This step is certified in Lean by the de Sitter PG average theorem in `StaticSanityCheck/DeSitterPG.lean`.

It is worth noting that the causal domain of the de Sitter foliation is bounded by the cosmological horizon at $r = H^{-1}$, so that $D_\Theta$ has finite volume. The infrared limit defining the constraint is therefore saturated at

12

a finite, geometrically determined scale. This is in sharp contrast with the Minkowski case, where $D_\Theta$ extends to spatial infinity and the unbounded growth of the integration volume drives $\langle K^2 \rangle$ to zero. The vacuum selection mechanism can thus be traced to this structural asymmetry: de Sitter spacetime possesses a natural causal scale at which the constraint is intrinsically satisfied, whereas Minkowski spacetime lacks any such scale.



**Figure 4:** Hybrid toy model sensitivity: a Minkowski-like interior matched to a de Sitter exterior with transition radius $r_{\text{trans}}$. The leafwise average $\langle K^2 \rangle$ converges to the de Sitter value once the infrared domain extends well beyond the transition scale ($R_{\text{max}} \gg r_{\text{trans}}$), illustrating infrared dominance of the vacuum selection rule in inhomogeneous settings.

The leafwise constraint therefore selects de Sitter spacetime as an admissible vacuum, with the expansion rate fixed by

$$H^2 = \frac{K_0^2}{3}. \tag{35}$$

In the Lean artifact, this selection rule is proved both in the direct de Sitter module and in an independent module obtained by substitution into the general $K^2$ expression. This relation fixes the curvature scale of the *asymptotic* vacuum geometry selected by the leafwise constraint. Since the constraint is formally defined in the infinite-volume limit ($R \to \infty$), it does not impose a constant Hubble rate during the dynamical history at finite causal volume, where standard General Relativity is recovered. In the present case, the constancy of $K^2$ over the maximal causal domain ensures that the asymptotic average coincides with the pointwise value, providing a robust realization of the selected vacuum. More generally, however, the constraint requires only the global infrared average and does not enforce pointwise constancy of the extrinsic curvature.

## 6.4 Infrared dominance of the leafwise constraint

At this stage a potential concern may arise. Since the leafwise constraint fixes a non-zero value of the normalized average $\langle K^2 \rangle_{D_\Theta}$, one might worry that local Schwarzschild or post-Newtonian physics could be incompatible with the theory. This concern, however, relies on an incorrect interpretation of the constraint as a local condition.

The geometric constraint does not act pointwise on $K^2$, but only through its leafwise average over a causally defined domain. As a result, its effect is controlled by the large-scale structure of the foliation rather than by local curvature near compact sources. In the following we show explicitly that, for physically relevant foliations, the induced geometry on the $\Theta = $ const hypersurfaces remains locally Euclidean, ensuring full compatibility with standard Schwarzschild and post-Newtonian physics. The corresponding IR-suppression statement for compactly supported contributions is formalized in Lean as the compact-support IR-dominance theorem in `StaticSanityCheck/IRDominance.lean`.

**Lemma 1** (Euclidean induced metric on the SdS–PG foliation). *Consider the static Schwarzschild–de Sitter line element*

$$ds^2 = A(r)\, dt^2 - B(r)\, dr^2 - r^2 d\Omega^2, \qquad A(r) = 1 - \frac{2M}{r} - H^2 r^2, B(r) = \frac{1}{A(r)}.$$
(36)

*Let the foliation be defined by the scalar field*

$$\Theta(t, r) = t + \psi(r),$$
(37)

*and choose the Painlevé–Gullstrand–type slicing*

$$\psi'(r) = \frac{\sqrt{\frac{2M}{r} + H^2 r^2}}{A(r)}.$$
(38)

*Then the metric induced on the hypersurfaces $\Sigma_\Theta : \Theta = $ const is exactly Euclidean:*

$$\gamma_{ij}\, dx^i dx^j = dr^2 + r^2 d\Omega^2, \qquad hence \qquad \sqrt{\gamma} = r^2 \sin\theta.$$
(39)

*Proof.* On a hypersurface $\Theta = $ const we have $d\Theta = dt + \psi'(r)\, dr = 0$, hence

$$dt = -\psi'(r)\, dr.$$
(40)

Substituting (40) into (36), the induced line element on $\Sigma_\Theta$ becomes

$$ds^2\big|_{\Sigma_\Theta} = \left(B(r) - A(r)\psi'(r)^2\right) dr^2 + r^2 d\Omega^2.$$
(41)

Using (38) and $B = 1/A$, we compute

$$B(r) - A(r)\psi'(r)^2 = \frac{1}{A(r)} - A(r) \frac{\frac{2M}{r} + H^2 r^2}{A(r)^2} = \frac{1 - \left(\frac{2M}{r} + H^2 r^2\right)}{A(r)}.$$
(42)

Finally, since $A(r) = 1 - \frac{2M}{r} - H^2 r^2$, the numerator in (42) equals $A(r)$ and therefore

$$B(r) - A(r)\psi'(r)^2 = \frac{A(r)}{A(r)} = 1. \tag{43}$$

Substituting (43) into (41) yields (39). $\qquad\square$

As a consequence, the leafwise geometric constraint is dominated by the large-scale structure of the foliation, while local Schwarzschild and post-Newtonian physics remain unaffected. The apparent tension between the constraint and local gravity is therefore resolved at the geometric level.

# 7 Covariance and preferred foliation backgrounds

The formalism is generally covariant at the level of the action, but backgrounds for which $\nabla_\mu \Theta$ is timelike naturally select a preferred foliation of spacetime. This mechanism is conceptually related to those appearing in Einstein–Æther theories [1], Hořava–Lifshitz gravity [7], and khronometric models [3].

Although the foliation is defined by the gradient of a scalar field, the present framework differs from khronometric and scalar Einstein–Æther theories in a crucial way. The field $\Theta$ is not introduced as an independent dynamical degree of freedom with its own kinetic couplings, but serves a purely geometric role in defining the hypersurfaces on which the global constraint acts. Related scalar-aether and khronometric constructions, used for comparison, are discussed for instance in [4, 8]. The scalar field $\Theta$ is not introduced as an independent propagating degree of freedom describing new local physics. Instead, it serves a geometric role in defining the preferred foliation on which the global constraint acts. While a kinetic term is included in the local action, its role is to ensure the timelike character and regularity of the foliation, rather than to introduce an additional dynamical scalar mode in the infrared regime considered here.

The breaking of local Lorentz symmetry is therefore spontaneous rather than fundamental. The action remains fully diffeomorphism invariant, while specific solutions dynamically single out a preferred time direction through the gradient of $\Theta$. In this sense, the preferred foliation does not represent a violation of covariance at the level of physical laws, but emerges as a property of the vacuum geometry selected by the leafwise constraint.

## 7.1 Homogeneous cosmology: minisuperspace consistency

As an internal consistency test of the constrained variational structure, one can reduce the theory to homogeneous FRW minisuperspace,

$$ds^2 = N(t)^2 \, dt^2 - a(t)^2 \, d\vec{x}^{\,2}. \tag{44}$$

In this sector the extrinsic-curvature invariant takes the simple form

$$K^2 = 3\left(\frac{\dot{a}}{aN}\right)^2,\tag{45}$$

and on a comoving ball one finds $I_1 = K^2 I_0$, hence $Q = I_1/I_0 = K^2$ identically. The leafwise constraint therefore yields the selection rule

$$H^2 \equiv \left(\frac{\dot{a}}{aN}\right)^2 = \frac{K_0^2}{3}.\tag{46}$$

The full minisuperspace Euler–Lagrange system (for $a$, $N$, $\lambda$) is consistent on the de Sitter branch, and the constraint propagates without drift. Moreover, the three minisuperspace equations satisfy an exact off-shell Noether/Bianchi-type identity reflecting time-reparametrization invariance,

$$E_a\,\dot{a} + E_N\,\dot{N} + E_\lambda\,\dot{\lambda} - \frac{d}{dt}(NE_N) - \frac{d}{dt}(\lambda E_\lambda) = 0,\tag{47}$$

which guarantees compatibility among the channels and structurally explains the observed constraint propagation. These results have been verified symbolically and numerically in notebooks 15–20 of the supplementary `Variational_Derivation` pipeline, with all residuals confirmed null to machine precision.

### 7.1.1 Barotropic matter on the hard-constrained FRW branch

As a further internal consistency check, we include an effective barotropic matter sector with equation of state $p = w\rho$ and energy density $\rho(a) = \rho_0 a^{-3(1+w)}$. In minisuperspace, the corresponding matter contribution is $-Na^3\rho(a) = -\rho_0 a^{-3w} N$. Working in the homogeneous reduction, the Lagrangian becomes

$$L = -\frac{3a\dot{a}^2}{\kappa N} - \frac{\Lambda a^3 N}{\kappa} + \lambda(t)\left(\frac{3a\dot{a}^2}{N^2} - K_0^2 a^3\right) - \rho_0 a^{-3w} N,$$

where in minisuperspace one may identify $\Theta = t$ (up to reparametrization), so a leafwise function $\lambda(\Theta)$ is represented as $\lambda(t)$ while remaining constant on each leaf.

On the hard-constrained homogeneous branch one has $Q = K^2$ identically, so the constraint channel yields

$$H^2 \equiv \left(\frac{\dot{a}}{aN}\right)^2 = \frac{K_0^2}{3}.$$

The lapse channel instead fixes the leafwise multiplier; on the de Sitter branch ($H = \text{const}$),

$$\lambda(t) = -\frac{1}{2}\frac{-K_0^2 + \Lambda + \kappa\rho_0\,e^{-3(1+w)Ht}}{K_0^2\kappa}, \qquad \dot{\lambda}(t) = \frac{3H\rho_0(1+w)}{2K_0^2}\,e^{-3(1+w)Ht}.$$

For $w = -1$ one recovers $\dot{\lambda} = 0$, while for $w \neq -1$ matter is encoded in $\lambda(t)$ rather than in an evolving $H(t)$. This reinforces the need for the finite-domain/causal prescription for realistic cosmological eras.

## 7.2 Perturbative spectrum (summary of supplementary results)

A dedicated supplementary pipeline (`Perturbative_Spectrum_Study`, scripts 00–15) analyzes the quadratic perturbative kernel around isotropic FRW/de Sitter backgrounds. The kernel is decomposed in Barnes–Rivers spin projectors, yielding separate spin-2 (tensor), spin-1 (vector), and a coupled spin-0 (scalar) block.

In the tensor sector the quadratic action takes the standard form

$$S_T^{(2)} \sim \int a^3 \left( G_T \dot{h}^2 - F_T \frac{(\nabla h)^2}{a^2} \right), \tag{48}$$

so ghost/gradient stability requires $G_T > 0$ and $F_T > 0$, with $c_T^2 = F_T/G_T$ approaching the GR value as non-local corrections scale as $1/I_0$. Analogously, in the vector sector one finds $c_V^2 = g_1/c_1$ with positivity conditions entirely parallel to the tensor case.

The scalar sector is described by a $2 \times 2$ kinetic matrix $K_s$ and gradient matrix $G_s$, so UV stability reduces to positive definiteness of $K_s$ and positivity of the eigenvalues of $K_s^{-1} G_s$ (including mixing). On the constrained FRW branch, the linear scalar channel is frozen in cosmic gauge, consistently with the minisuperspace structure and with the interpretation of $\Theta$ as a geometric time-ordering field rather than an additional propagating infrared degree of freedom.

Across all channels, the supplementary analysis verifies that non-local contributions to the quadratic coefficients are infrared-suppressed (scaling as $I_0^{-1}$) and that the full dispersion relations match the expected UV limits. Complete derivations, explicit coefficient expressions, and numerical spot-checks are available in the pipeline logs (`logs/*.log`) and notebooks, with the normalized-channel second-variation identities summarized in Appendix A.6 and the isotropic spin-projector inversion summarized in Appendix B.

## 8 Computational details

Symbolic computations underlying the results of this work were performed using *Wolfram Mathematica* v. 14.3. Additional numerical analyses and consistency checks of the infrared scaling behaviour were carried out using Python-based routines. The calculations are organized in a sequence of notebooks implementing independent checks of the geometric invariants,

the local action, and the evaluation of the leafwise constraint in symmetric settings:

1. `00_Setup_Assumptions.nb` - Global assumptions and symbol definitions.

2. `01_Invariants_X_K2_R.nb` - Computation of $X$, $K^2$, and $R$ from the metric ansatz.

3. `02_Action_Lagrangian.nb` - Construction of the local four-dimensional Lagrangian and of the leafwise constraint functional.

4. `03_Leff_Radial_Reduction.nb` - Angular integration and construction of the radial kernels entering the leafwise averages.

5. `04_SanityChecks.nb` - Verification of limiting cases (Schwarzschild, $\psi' = 0$).

6. `05_Test_Minkowski.nb` - Evaluation of the leafwise average in Minkowski spacetime and analysis of its infrared behaviour.

7. `06_Test_deSitter.nb` - Verification that de Sitter spacetime satisfies the leafwise constraint through a cosmological (Painlevé–Gullstrand) slicing.

8. `07_Domain_sensitivity_calculations.py` - In addition to symbolic checks, quantitative sensitivity analyses were performed (using Python/SciPy) to verify the asymptotic scaling behavior of $\langle K^2 \rangle$ and the convergence rate of the integrals in the limit $R \to \infty$.

An additional notebook, `GR_Spherical_Foliation_K2_R.nb`, provides an independent derivation of the geometric invariants through explicit construction of the Christoffel symbols, Riemann tensor, and extrinsic curvature tensor $K_{\mu\nu}$.

The notebooks are provided as supplementary material.

In addition, a dedicated supplementary pipeline (`Paper/Variational_Derivation`) provides a complete derivation of the non-local variational structure (including explicit boundary/shape terms and a covariant causal-domain formulation), organized as scripts 00–25 with mandatory checks. The pipeline is executable via `wolframscript` and produces both notebooks and plain-text logs (`logs/*.log`) for reproducibility.

A second dedicated supplementary pipeline (`Paper/Perturbative_Spectrum_Study`) provides the perturbative spectrum analysis (ghost/gradient conditions and dispersion relations in tensor/vector/scalar sectors, including scalar mixing), the quadratic non-local kernel from second variations of $Q = I_1/I_0$, and second-order boundary shape-derivative terms. The pipeline is organized as scripts 00–15 with mandatory checks and plain-text logs for reproducibility.

A third dedicated supplementary pipeline (`Paper/Barotropic_Cosmology_Study`) provides minisuperspace FRW checks with barotropic matter. The validated block (`00_barotropic_hard_constraint_consistency.wl`) enforces the hard branch $H^2 = K_0^2/3$ and solves the lapse channel for $\lambda(t)$, with mandatory checks (`check=True`) recorded in plain-text logs for reproducibility.

## 8.1 Formal verification artifact (Lean)

The Lean formalization used in this work is publicly available and version-pinned for reproducibility:

- Repository: GitHub repository

- Artifact release used for this manuscript: v2.0 release snapshot

- Archived DOI: 10.5281/zenodo.18361297

- Continuous integration build: CI workflow

For referee traceability, the artifact README provides a mapping from paper equations to Lean theorems, with assumptions: README traceability table.

## 8.2 Scope of formal verification (explicit boundaries)

For precision, we state explicitly what is and is not currently certified in the Lean development associated with this work.

**Starting point for $K^2$.** The Lean proofs certify the full analytic chain *starting from* the explicit coordinate expression

$$K^2_{\text{general}} = \frac{\text{NumK2}}{\text{DenK2}},$$

and all substitutions/limits built on top of it (Minkowski IR scaling, de Sitter selection, abstract averaging lemmas, and IR-dominance statements). At present, the Lean code does *not* yet include a complete differential-geometric derivation of this coordinate formula from first principles ($u^\mu$, projectors, connection, and tensorial construction of $K_{\mu\nu}K^{\mu\nu}$).

**Causal domain $D_\Theta$.** In Lean, the causal domains are formalized via nested proxy families suitable for infrared analysis (balls $B_R$, and in de Sitter $B_{\min(R,H^{-1})}$), for which well-posedness, positivity of the normalization denominator, and finite-radius saturation are proved. What is not yet formalized is the full Lorentzian definition of mutual causal reachability and

a general theorem proving equivalence between that definition and the proxy domains in all backgrounds.

Accordingly, statements of formal certification should be read with the following canonical scope: *The Lean artifact verifies the analytic chain of results starting from the explicit coordinate expression $K^2_{general}$ and the proxy domains used in the manuscript; it does not yet certify the derivation of $K^2_{general}$ from the full geometric definition $K_{\mu\nu}K^{\mu\nu}$, nor the equivalence between the proxy domains and the general Lorentzian causal-domain definition.*

**Reproducibility note.** Build verified for artifact release `v2.0` with Lean `v4.27.0` / mathlib `a3a10db0e9d66acbebf76c5e6a135066525ac900`; CI reproduces `lake build` on every push.

**Variational structure (supplementary).** The full bulk+boundary variational derivation of the non-local term, including explicit shape derivatives for finite/causal domains and a covariant indicator-function formulation, is verified in the supplementary Mathematica pipeline (`Variational_Derivation`, scripts 00–25). This verification is symbolic plus independently cross-checked numerically at machine precision; it is complementary to (and currently separate from) the Lean formalization scope stated above.

# 9   Conclusion

We have presented a scalar-field framework in which the foliation defined by the gradient of $\Theta$ is subject to a non-local geometric constraint acting leafwise on spacetime hypersurfaces. The constraint fixes the asymptotic value of the normalized average of the squared extrinsic curvature in the infrared limit, rather than imposing a pointwise condition on the geometry.

While the theory locally reproduces the field equations of General Relativity when the foliation aligns with static time coordinates, the asymptotic constraint leads to a non-trivial selection of the vacuum structure. Asymptotically flat Minkowski spacetime is excluded as a vacuum solution because its leafwise average vanishes in the infrared limit (scaling as $R^{-2}$), whereas de Sitter spacetime emerges as a consistent asymptotic solution with curvature scale fixed by the geometric selection rule

$$H^2 = \frac{K_0^2}{3}. \tag{49}$$

Because the constraint is defined as a limit at infinity $(R \to \infty)$, it acts as a boundary condition on the foliation. Local matter distributions and compact objects contribute only at measure-zero to the infinite-volume average, ensuring that standard Schwarzschild and post-Newtonian physics

are fully recovered without introducing unsuppressed local modifications or additional forces.

The present framework is intended as a proof-of-principle for vacuum selection in the strict infrared regime. A complete cosmological implementation requires a finite-domain prescription for the causal regions $D_\Theta$. We anticipate that the resulting finite-volume corrections—suppressed in the early universe but relevant at late times—will provide the dynamical mechanism driving the evolution toward the selected de Sitter vacuum. Developing such a finite-domain formulation and its implications for the radiation- and matter-dominated eras is left for future work. This necessity is reinforced by the barotropic minisuperspace check: under a uniform hard implementation the homogeneous branch remains de Sitter, while the matter sector is absorbed into the leafwise multiplier $\lambda(\Theta)$ rather than reopening a standard FRW evolution $H(t)$.

These results suggest that the observed late-time cosmic acceleration may reflect a global geometric property of the spacetime foliation defining the present—a resistance to staticity enforced at the cosmological horizon—rather than requiring the introduction of an additional dynamical dark energy degree of freedom.

# References

[1] Ted Jacobson and David Mattingly. Gravity with a dynamical preferred frame. *Phys. Rev. D*, 64:024028, 2001.

[2] Ted Jacobson and David Mattingly. Static post-newtonian equivalence of general relativity and gravity with a dynamical preferred frame. *Phys. Rev. D*, 69:064005, 2004.

[3] Diego Blas, Oriol Pujolàs, and Sergey Sibiryakov. Consistent extension of hořava gravity. *Phys. Rev. Lett.*, 104:181302, 2010.

[4] Ted Jacobson and Eugene Lim. The scalar einstein-Æther theory. *Phys. Rev. D*, 90:024014, 2014.

[5] S.-Y. Pi. Space-times produced by a time-dependent scalar field. 2005.

[6] Nemanja Kaloper and Antonio Padilla. Vacuum energy sequestering: The framework and its cosmological consequences. *Phys. Rev. D*, 90:084023, 2014.

[7] Petr Hořava. Quantum gravity at a lifshitz point. *Phys. Rev. D*, 79:084008, 2009.

[8] Diego Blas et al. Slowly moving black holes in lorentz-violating scalar-tensor gravity. *Phys. Rev. D*, 111:024062, 2024.

# A  Covariant causal-domain variation and boundary terms

This appendix makes explicit the bulk+boundary variational structure of the leafwise non-local functional entering the action (16). The key point is that the causal domain on each leaf is geometrically defined and therefore varies under field variations. This produces boundary/shape terms that can be written covariantly using an indicator function.

## A.1  Covariant representation of leafwise functionals

Let $\Theta$ be a scalar field with timelike gradient ($X \equiv g^{\mu\nu}\partial_\mu\Theta\partial_\nu\Theta > 0$) defining the foliation $\Sigma_\theta : \Theta = \theta$ with unit normal $u_\mu = \partial_\mu\Theta/\sqrt{X}$ and induced metric $h_{\mu\nu} = g_{\mu\nu} - u_\mu u_\nu$. Let $K_{\mu\nu}$ be the extrinsic curvature of $\Sigma_\theta$ and $K^2 \equiv K_{\mu\nu}K^{\mu\nu}$.

We define a (possibly trivial) leafwise weight $W$ and introduce the covariant leaf measure density

$$\mu(x;\theta) \equiv \sqrt{-g}\,W(x)\,\sqrt{X}\,\delta(\Theta(x) - \theta). \tag{50}$$

Using standard $\delta$-function identities for level sets, one has

$$\int d^4x\,\mu(x;\theta)\,F(x) = \int_{\Sigma_\theta} d^3x\,\sqrt{\gamma}\,W\,F\big|_{\Sigma_\theta}. \tag{51}$$

Let $D_\theta \subset \Sigma_\theta$ denote the (causally defined) integration region on the leaf. We represent it by an indicator function $\chi_\theta(x) \in \{0,1\}$ supported on $D_\theta$: $\chi_\theta(x) = 1$ for $x \in D_\theta$ and $\chi_\theta(x) = 0$ otherwise. Then the leafwise functionals can be written as

$$I_0[\theta] \equiv \int d^4x\,\mu(x;\theta)\,\chi_\theta(x), \tag{52}$$

$$I_1[\theta] \equiv \int d^4x\,\mu(x;\theta)\,\chi_\theta(x)\,K^2(x), \tag{53}$$

$$Q[\theta] \equiv \frac{I_1[\theta]}{I_0[\theta]} = \langle K^2\rangle_{D_\theta}. \tag{54}$$

## A.2  First variations: bulk and boundary channels

Consider an arbitrary first-order variation of the fields and the domain data,

$$\begin{aligned}
g_{\mu\nu} &\to g_{\mu\nu} + \varepsilon\,\delta g_{\mu\nu}, & \Theta &\to \Theta + \varepsilon\,\delta\Theta, \\
\chi_\theta &\to \chi_\theta + \varepsilon\,\delta\chi_\theta, & K^2 &\to K^2 + \varepsilon\,\delta K^2.
\end{aligned} \tag{55}$$

At integrand level, the variations of the covariant densities are exactly

$$\delta(\mu\,\chi_\theta) = \chi_\theta\,\delta\mu + \mu\,\delta\chi_\theta, \tag{56}$$

$$\delta\big(\mu\,\chi_\theta\,K^2\big) = \chi_\theta\,K^2\,\delta\mu + \chi_\theta\,\mu\,\delta K^2 + \mu\,K^2\,\delta\chi_\theta. \tag{57}$$

Therefore,

$$\delta I_0 = \delta I_0^{\text{bulk}} + \delta I_0^{\partial D}, \qquad \delta I_0^{\text{bulk}} \equiv \int d^4x \, \chi_\theta \, \delta\mu, \qquad \delta I_0^{\partial D} \equiv \int d^4x \, \mu \, \delta\chi_\theta,$$
$$\tag{58}$$

$$\delta I_1 = \delta I_1^{\text{bulk}} + \delta I_1^{\partial D},$$
$$\delta I_1^{\text{bulk}} \equiv \int d^4x \, \chi_\theta ( K^2 \, \delta\mu + \mu \, \delta K^2 ), \quad \delta I_1^{\partial D} \equiv \int d^4x \, \mu \, K^2 \, \delta\chi_\theta. \tag{59}$$

The ratio functional satisfies the exact identity

$$\delta Q = \frac{I_0 \, \delta I_1 - I_1 \, \delta I_0}{I_0^2}. \tag{60}$$

Using the split (58)–(59), the boundary contribution is

$$\delta Q\big|_{\partial D} = \frac{I_0 \, \delta I_1^{\partial D} - I_1 \, \delta I_0^{\partial D}}{I_0^2}. \tag{61}$$

If the domain variation can be parameterized by an infinitesimal displacement $\varepsilon \, \xi$ of the boundary $\partial D_\theta$ (shape variation), one may write

$$\delta I_0^{\partial D} \equiv b_0 \, \xi, \qquad \delta I_1^{\partial D} \equiv b_1 \, \xi, \tag{62}$$

leading to the compact form

$$\delta Q\big|_{\partial D} = \frac{b_1 I_0 - b_0 I_1}{I_0^2} \, \xi. \tag{63}$$

This is the universal boundary structure in the normalized channel.

## A.3  Shape derivatives from an indicator: first and second order

To make the domain-variation channel explicit, consider a one-parameter family of domains defined by a moving radial boundary

$$r = R + \varepsilon \, \rho + \frac{\varepsilon^2}{2} \sigma,$$

encoded by an indicator

$$\chi_\varepsilon(r) = H\left( R + \varepsilon\rho + \frac{\varepsilon^2}{2}\sigma - r \right),$$

with $H$ the Heaviside step function. Differentiating distributionally yields

$$\delta\chi \equiv \frac{d\chi_\varepsilon}{d\varepsilon}\bigg|_{\varepsilon=0} = \rho \, \delta(R - r), \tag{64}$$

23

and

$$\delta^2\chi \equiv \frac{d^2\chi_\varepsilon}{d\varepsilon^2}\bigg|_{\varepsilon=0} = \sigma\,\delta(R-r) + \rho^2\,\delta'(R-r), \tag{65}$$

where $\delta'$ is the derivative of the Dirac delta with respect to its argument.

Inserting these expressions into the covariant representations (58)–(59) reproduces the Leibniz-rule differentiation of integrals with moving boundary, both at first and second order. In particular, the second-order boundary contribution is not postulated: it follows uniquely from the domain dependence encoded in $\chi_\varepsilon$. The identity (65) has been verified analytically and independently cross-checked numerically to residuals of order $10^{-12}$ in the supplementary pipeline logs.

## A.4 Variation of the non-local leafwise action

The non-local part of the action can be written as

$$S_{\mathrm{NL}} = \int d\theta\,\lambda(\theta)\left(I_1[\theta] - K_0^2 I_0[\theta]\right). \tag{66}$$

Under $\lambda \to \lambda + \varepsilon\eta$ and the field/domain variations above, one finds

$$\delta S_{\mathrm{NL}} = \int d\theta\left[\eta(\theta)\left(I_1 - K_0^2 I_0\right) + \lambda(\theta)\left(\delta I_1 - K_0^2\delta I_0\right)\right]. \tag{67}$$

The first term enforces the leafwise constraint $I_1 - K_0^2 I_0 = 0$. The second term contains the geometric response and splits into bulk and boundary pieces according to (58)–(59). In particular, the boundary channel contributes

$$\delta S_{\mathrm{NL}}\big|_{\partial D} = \int d\theta\,\lambda(\theta)\left(\delta I_1^{\partial D} - K_0^2\delta I_0^{\partial D}\right), \tag{68}$$

with $\delta I_a^{\partial D}$ computable from (64) in explicit domain models.

## A.5 Infrared suppression in the normalized channel

Finally, the exact ratio identity (60) implies that, for variations whose bulk contributions scale extensively with the domain size (schematically $\delta I_a = \mathcal{O}(I_0)$), the induced correction in the normalized channel scales as

$$\delta Q = \mathcal{O}\left(\frac{1}{I_0}\right), \tag{69}$$

so local modifications to the field equations are parametrically suppressed by the infrared volume of the causal domain. This provides a precise underpinning for the infrared-dominance arguments used in the main text.

### A.6 Second variations of the normalized channel and quadratic kernel

For the normalized leafwise functional $Q = I_1/I_0$, consider the second-order expansion

$$I_a(\varepsilon) = I_a + \varepsilon\,\delta I_a + \frac{\varepsilon^2}{2}\,\delta^2 I_a, \qquad (a = 0, 1),$$

and define

$$Q(\varepsilon) = \frac{I_1(\varepsilon)}{I_0(\varepsilon)} = Q + \varepsilon\,q_1 + \frac{\varepsilon^2}{2}\,q_2 + O(\varepsilon^3).$$

A direct ratio expansion gives the exact identities

$$q_1 = \frac{I_0\,\delta I_1 - I_1\,\delta I_0}{I_0^2}, \tag{70}$$

and

$$q_2 = \frac{-2\,\delta I_0\,\delta I_1\,I_0 + 2(\delta I_0)^2 I_1 + I_0\big(\delta^2 I_1\,I_0 - \delta^2 I_0\,I_1\big)}{I_0^3}. \tag{71}$$

On the constrained branch $I_1 = Q\,I_0$ these simplify to

$$q_1 = \frac{\delta I_1 - Q\,\delta I_0}{I_0}, \qquad q_2 = \frac{\delta^2 I_1 - Q\,\delta^2 I_0}{I_0} - \frac{2\,\delta I_0\,(\delta I_1 - Q\,\delta I_0)}{I_0^2}. \tag{72}$$

Therefore, for extensive variations $\delta I_a = O(I_0)$ and $\delta^2 I_a = O(I_0)$, both $q_1$ and $q_2$ are infrared-suppressed, scaling as $O(1/I_0)$. This provides the algebraic backbone needed to construct the quadratic non-local kernel used in the supplementary `Perturbative_Spectrum_Study` pipeline.

## B  Barnes–Rivers decomposition and closed-form inversion

For an isotropic quadratic operator acting on symmetric rank-2 perturbations, it is convenient to decompose the kernel into Barnes–Rivers spin projectors

$$\mathcal{O} = c_2 P^{(2)} + c_1 P^{(1)} + c_s P^{(0s)} + c_w P^{(0w)} + c_m\Big(P^{(0sw)} + P^{(0ws)}\Big), \tag{73}$$

where $P^{(2)}$, $P^{(1)}$ project onto the spin-2 and spin-1 subspaces, while the spin-0 sector is represented by the coupled block spanned by $P^{(0s)}$, $P^{(0w)}$ with mixing $c_m$. The scalar-block determinant is

$$\det S \equiv c_s c_w - c_m^2. \tag{74}$$

Whenever $c_2 \neq 0$, $c_1 \neq 0$ and $\det S \neq 0$, the inverse operator exists and takes the closed form

$$\mathcal{O}^{-1} = \frac{1}{c_2}P^{(2)} + \frac{1}{c_1}P^{(1)} + \frac{c_w P^{(0s)} + c_s P^{(0w)} - c_m\big(P^{(0sw)} + P^{(0ws)}\big)}{c_s c_w - c_m^2}. \tag{75}$$

This decomposition makes explicit that (in the isotropic case) tensor and vector channels do not mix with the scalar block, and that stability/invertibility conditions reduce to positivity of the relevant coefficients and of $\det S$. These identities are verified analytically in the supplementary `Perturbative_Spectrum_Study` pipeline (projector algebra, scripts 07, and bilateral inversion including IR limits, script 12).